

Organic Complementary Inverters Based on Inverted Coplanar Thin-Film Transistors Employing Different Contact Functionalization

Sabrina Steffens¹, Hagen Klauk¹

S.Steffens@fkf.mpg.de

¹Max Planck Institute for Solid State Research, Organic Electronics, Heisenbergstr. 1 70569 Stuttgart, Germany
Keywords: Complementary inverter, Bottom-contact TFTs, Contact functionalization, Flexible substrate, PhC₂-BQQDI

ABSTRACT

Organic complementary inverters based on inverted coplanar organic TFTs employing two vacuum-deposited small-molecule semiconductors were fabricated on flexible substrates. The source and drain contacts of the TFTs were functionalized with pentafluorobenzenethiol (PFBT) or 4-(methylsulfanyl)-thiophenol (MeSTP). For the optimum combination of materials, the inverters have characteristic signal-delay time constants below 2 μ s at a supply voltage of 2 V.

1 Introduction

Organic semiconductors provide the possibility to fabricate electronic systems, such as information displays, radio-frequency identification tags and biocompatible diagnostic devices, on flexible polymeric substrates and paper, since organic semiconductors can be deposited at or near room temperature, in contrast to common inorganic semiconductors. For mobile electronics systems, a low power consumption is a prerequisite. Therefore, the complementary circuit design is favored, since it results in a significantly smaller static power consumption, a greater noise immunity, a larger small-signal gain, and a larger output swing compared to the unipolar circuit design.[1],[2]

Organic complementary circuits are typically based on p-channel and n-channel TFTs fabricated using two different organic semiconductors that favor the injection and transport of either positive or negative charge carriers, respectively. While organic p-channel TFTs already have a good performance, with contact resistances as small as 10 Ω cm,[3][4] subthreshold swings at the physical limit (59 mVdecade⁻¹),[5] and excellent long-term stability, there is still a need to improve the performance of n-channel organic TFTs. So far, the contact resistances reported for n-channel organic TFTs are rarely below 1 k Ω cm.[6]

The contact resistance of organic TFTs fabricated in the inverted coplanar (bottom-gate, bottom-contact) device architecture can be improved by functionalizing the surface of the source/drain (S/D) contacts with a chemisorbed monolayer of an appropriate thiol.

For p-channel organic TFTs, pentafluorobenzenethiol (PFBT) has emerged as the most promising thiol for this purpose.[7] while for n-channel TFTs, 4-(methylsulfanyl)-thiophenol (MeSTP) has shown excellent results.[8]

For organic complementary circuits, the challenge is to find a way to functionalize the S/D contacts of the p-channel and n-channel TFTs with different thiols despite both being present on the same substrate. Here we compare the static and dynamic performance of two different organic complementary inverters, one in which the S/D contacts of the p-channel and n-channel TFTs were functionalized using the same thiol (PFBT), and one in which the S/D contacts of the n-channel TFTs were functionalized using MeSTP and those of the p-channel TFTs with PFBT.

2 Experiment

All TFTs and inverters were fabricated on 125- μ m-thick flexible polyethylene naphthalate (PEN) substrates. The TFTs were fabricated in the inverted coplanar (bottom-gate, bottom-contact) device architecture. For all TFTs, aluminum gate electrodes were deposited by thermal evaporation in vacuum and patterned using a silicon stencil mask. The aluminum surface was exposed to oxygen plasma to form a thin aluminum oxide layer, followed by immersing the substrates into a 2-propanol solution of *n*-tetradecylphosphonic acid for 3 to 4 hours at room temperature to form a self-assembled monolayer (SAM) on the AlO_x surface. The hybrid AlO_x/SAM gate dielectric has a total thickness of 8 nm and a unit-area capacitance (C_{diel}) of 0.6 μ Fcm⁻². Gold source and drain (S/D) contacts with a thickness of 30 nm were deposited by thermal evaporation in vacuum and patterned using a stencil mask.

Two substrates were fabricated: On substrate A, the same thiol (PFBT) was used to functionalize the S/D contacts of both the p-channel and the n-channel TFTs. On substrate B, the S/D contacts of the n-channel TFTs were functionalized using MeSTP, and those of the p-channel TFTs were functionalized using PFBT.

Substrate A: The Au S/D contacts of all TFTs were deposited and patterned using a stencil mask. The substrate was then immersed into a 10-mM ethanol solution of PFBT for 1 hour to form a chemisorbed PFBT monolayer on the surface of the S/D contacts of all TFTs, with the goal of minimizing the contact resistance of all TFTs.

Substrate B: The S/D contacts of the n-channel TFTs were deposited and patterned using a stencil mask that contains only the S/D patterns for the n-channel TFTs. The substrate was then immersed into a solution of MeSTP for 5 hours to minimize the contact resistance of the n-channel TFTs. Afterwards, the S/D contacts of the p-channel TFTs were deposited and patterned using a stencil mask containing only the S/D patterns for the p-channel TFTs, followed by immersing the substrate into a solution of PFBT for 1 hour to minimize the contact resistance of the p-channel TFTs.

On both substrates, the two semiconductors were then deposited, first the semiconductor for the n-channel TFTs (diphenylethyl-3,4,9,10-benzo[de]isoquinolino[1,8-gh]quinolinetetracarboxylic diimide; PhC₂-BQQDI), [9] followed by the semiconductor for the p-channel TFTs (dinaphtho[2,3-b:2',3'-f]thieno[3,2-b]thiophene; DNTT). [10] Each of the two semiconductors was patterned using one of two dedicated stencil masks. During the semiconductor depositions, the substrate was held at a temperature of 140 °C (PhC₂-BQQDI) or 80 °C (DNTT).

All TFTs have a channel length of 4 μm. The p-channel TFTs have a channel width of 20, 40 or 60 μm. In each inverter, the channel width of the n-channel TFTs is twice as large as that of the p-channel TFTs to compensate for the smaller channel-width-normalized transconductance of the n-channel organic TFTs. The transfer characteristics of the inverters were measured using an Agilent 4156C Precision Semiconductor Parameter Analyzer, controlled using the software "SweepMe!" (<https://sweep-me.net>). The dynamic measurements were performed using a GGB Industries Picoprobe Model 19C, a Tektronix TDS1000 oscilloscope and a Femto DPLCA-200 low-noise transimpedance amplifier. All electrical measurements were performed in ambient air at room temperature (20 °C, relative humidity 30-60 %) under yellow laboratory light.

3 Results and Discussion

On **substrate A**, the S/D contacts of the p-channel DNTT TFTs and those of the n-channel PhC₂-BQQDI TFTs were functionalized using the same thiol, PFBT. Based on previous work, PFBT is expected to have an advantageous effect on the contact resistance of the p-channel TFTs, but not necessarily on that of the n-channel TFTs.

However, using the same thiol for both the p-channel and the n-channel TFTs greatly simplifies the fabrication process.

Fig. 1 shows the measured static transfer characteristics of an inverter based on TFTs functionalized using PFBT. The inverter exhibits a full output-voltage swing between 0 V and the supply voltage V_{DD} (here: 2 V). The hysteresis in the transfer characteristics of the inverter is due to the hysteresis in the transfer characteristic of the n-channel PhC₂-BQQDI TFT. The transfer curve of the inverter shows a sharp transition with a maximum small-signal gain of 600; this is the largest small-signal gain reported for organic complementary inverters fabricated on flexible substrates. (For organic complementary inverters on glass substrates, a small-signal gain of 1600 has been reported. [11]) The switching voltage is close to half the supply voltage, and the effective noise margin is 80% of half the supply voltage, which is close to the best values reported in literature [11]–[17]. The static currents are no greater than 1 pA, which means that the static power consumption is no greater than 2 pW. A low power consumption is extremely important, particularly for mobile or wearable systems.

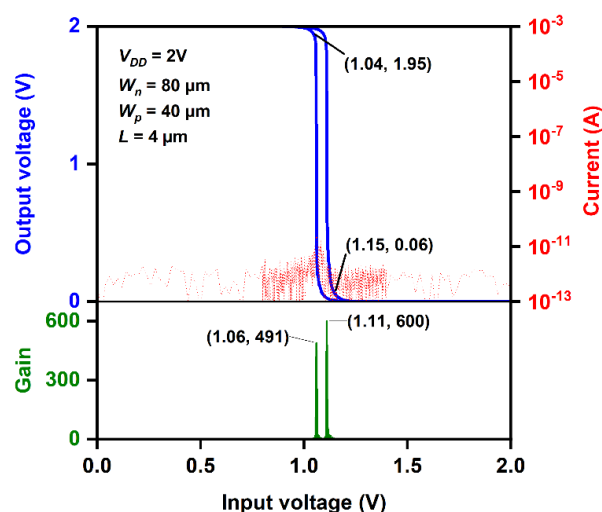


Fig 1. Measured static transfer characteristics of an organic complementary inverter based on a p-channel DNTT TFT and an n-channel PhC₂-BQQDI TFT whose source and drain contacts were functionalized using PFBT. The output voltage and the small-signal gain are plotted as a function of the input voltage for a supply voltage of 2 V.

As expected, the dynamic performance of the inverter is primarily limited by the n-channel TFT (see Figure 2). Nevertheless, at supply voltages above 2 V, the fall time of the inverter (the time it takes to discharge the output node through the n-channel TFT) approaches the rise time (the

time it takes to charge the output node through the p-channel TFT), even though the S/D contacts of the n-channel TFTs were not functionalized with the best-suited thiol. For a supply voltage of 3 V, the inverter switches with a rise time of 0.3 μs and a fall time of 4 μs .

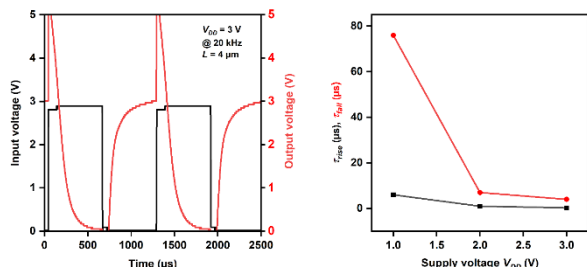


Fig 2. Dynamic performance of a complementary inverter based on a p-channel DNTT TFT and an n-channel PhC₂-BQQDI TFT whose source and drain contacts were functionalized using PFBT.

On substrate B, the process flow illustrated in Fig. 3 was carried out to functionalize the S/D contacts of the n-channel TFTs using MeSTP and those of the p-channel TFTs using PFBT.

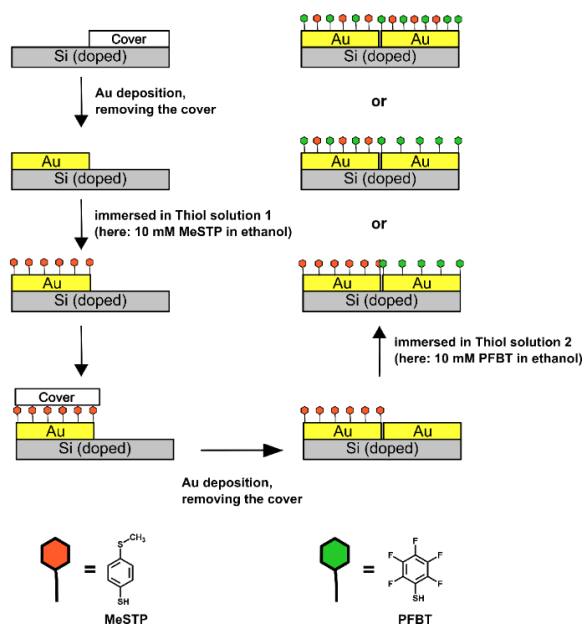


Fig 3. Sequential deposition of source/drain contacts and contact functionalization with MeSTP and PFBT.

The measured static transfer characteristic of an organic complementary inverter on substrate B fabricated following the scheme in Fig. 3 is shown in Fig. 4. The hysteresis in the measured transfer curves is significantly smaller (20 mV) compared to the inverter on substrate A (50 mV)

where the S/D contacts of all TFTs were functionalized using the same thiol (PFBT).

The transfer characteristic shows the full output swing and a sharp transition between the two static states with a small-signal gain of approximately 100. The effective noise margin is 70 % of half the supply voltage. The static current is below 2 pA, so the static power consumption is below 4 pW.

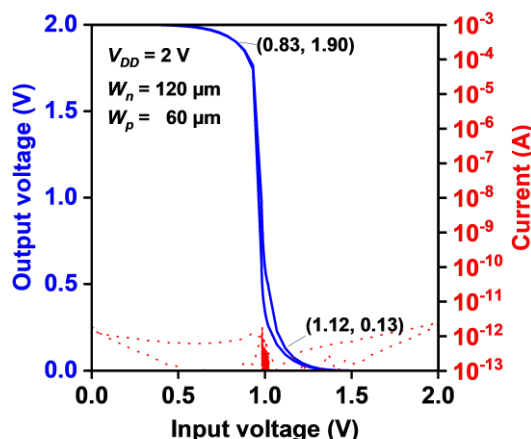


Fig 4. Static voltage transfer characteristic of an organic complementary inverter fabricated following the scheme in Figure 3.

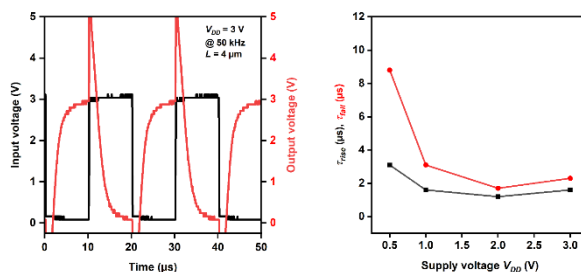


Fig 5. Dynamic performance of a complementary inverter. Source and drain contacts were functionalized with the thiol PFBT or MeSTP according to Figure 3.

For a supply voltage of 2 V, the inverter on substrate B switches with a rise time of 1.2 μs and a fall time of 1.7 μs (compared to a rise time of 0.3 μs and a fall time of 4 μs on substrate A). Therefore, the rise time (which is determined by the performance of the p-channel TFT) is shorter on substrate A (where the S/D contacts of the p-channel TFT were functionalized with the best possible thiol, PFBT), whereas the fall time (determined by the performance of the n-channel TFT) is shorter on substrate B (where the S/D contacts of the n-channel TFT were functionalized with the best possible thiol, MeSTP).

These results confirm that functionalizing the surface of the S/D contacts in bottom-gate, bottom-contact organic TFTs with the best-suited thiol (here: PFBT for the p-channel TFTs, MeSTP for the n-channel TFTs) greatly improves the dynamic performance of the TFTs and of integrated circuits based on them.

4 Conclusions

We demonstrated a method to functionalize the source and drain contacts of p-channel and n-channel thin-film transistors (TFTs) with different thiols in organic complementary inverters. Furthermore, we compared the static and dynamic performance of two different organic complementary inverters, one in which the S/D contacts of the p-channel and n-channel TFTs were functionalized using the same thiol (PFBT), and one in which the S/D contacts of the n-channel TFTs were functionalized using MeSTP and those of the p-channel TFTs with PFBT. Inverters based on the latter combination of materials exhibited a reduced hysteresis and an improved dynamic performance, demonstrating the importance of employing appropriate contact functionalization for both the p-channel and the n-channel TFTs used in complementary circuits.

References

- [1] H. Klauk, "Organic thin-film transistors," *Chem. Soc. Rev.*, vol. 39, no. 7, pp. 2643–2666, 2010.
- [2] T. Leydecker, Z. M. Wang, F. Torricelli, and E. Orgiu, "Organic-based inverters: Basic concepts, materials, novel architectures and applications," *Chem. Soc. Rev.*, vol. 49, no. 21, pp. 7627–7670, 2020.
- [3] J. Zeng *et al.*, "Ultralow contact resistance in organic transistors via orbital hybridization," *Nat. Commun.*, vol. 14, no. 1, pp. 1–10, 2023.
- [4] J. W. Borchert *et al.*, "Flexible low-voltage high-frequency organic thin-film transistors," *Sci. Adv.*, vol. 6, no. 21, p. eaaz5156, May 2020.
- [5] M. Geiger *et al.*, "Subthreshold Swing of 59 mV decade⁻¹ in Nanoscale Flexible Ultralow-Voltage Organic Transistors," *Adv. Electron. Mater.*, p. 2101215, 2022.
- [6] M. Uno *et al.*, "Short-Channel Solution-Processed Organic Semiconductor Transistors and their Application in High-Speed Organic Complementary Circuits and Organic Rectifiers," *Adv. Electron. Mater.*, vol. 1, no. 12, p. 1500178, 2015.
- [7] J. W. Borchert, R. T. Weitz, S. Ludwigs, and H. Klauk, "A Critical Outlook for the Pursuit of Lower Contact Resistance in Organic Transistors," *Adv. Mater.*, vol. 34, no. 2, p. 2104075, 2022.
- [8] T. Wollandt *et al.*, "Reliability of the Transmission Line Method and Reproducibility of the Measured Contact Resistance of Organic Thin-Film Transistors," 2025.
- [9] T. Okamoto *et al.*, "Robust, high-performance n-type organic semiconductors," *Sci. Adv.*, vol. 6, no. 18, p. eaaz0632, May 2020.
- [10] K. Niimi, M. J. Kang, E. Miyazaki, I. Osaka, and K. Takimiya, "General Synthesis of Derivatives," *Org. Lett.*, vol. 13, no. 13, pp. 3430–3433, 2011.
- [11] A. Petritz, A. Wolfberger, A. Fian, T. Griesser, M. Irimia-Vladu, and B. Stadlober, "Cellulose-Derivative-Based Gate Dielectric for High-Performance Organic Complementary Inverters," *Adv. Mater.*, vol. 27, no. 46, pp. 7645–7656, 2015.
- [12] A. Petritz *et al.*, "Cellulose as biodegradable high-k dielectric layer in organic complementary inverters," *Appl. Phys. Lett.*, vol. 103, no. 15, 2013.
- [13] J. B. Kim, C. Fuentes-Hernandez, S. J. Kim, S. Choi, and B. Kippelen, "Flexible hybrid complementary inverters with high gain and balanced noise margins using pentacene and amorphous InGaZnO thin-film transistors," *Org. Electron.*, vol. 11, no. 6, pp. 1074–1078, 2010.
- [14] T. H. Huang, H. C. Lai, B. J. Tzeng, and Z. Pei, "Air stable organic complementary inverter with high and balance noise margin based on polymer/metal oxide hybrid gate dielectrics," *Org. Electron.*, vol. 13, no. 8, pp. 1365–1369, 2012.
- [15] U. Zschieschang, F. Ante, M. Schlörholz, M. Schmidt, K. Kern, and H. Klauk, "Mixed self-assembled monolayer gate dielectrics for continuous threshold voltage control in organic transistors and circuits," *Adv. Mater.*, vol. 22, no. 40, pp. 4489–4493, 2010.
- [16] X. H. Zhang, W. J. Potscavage, S. Choi, and B. Kippelen, "Low-voltage flexible organic complementary inverters with high noise margin and high dc gain," *Appl. Phys. Lett.*, vol. 94, no. 4, pp. 92–95, 2009.
- [17] S. Tatemichi, M. Ichikawa, S. Kato, T. Koyama, and Y. Taniguchi, "Low-voltage, high-gain, and high-mobility organic complementary inverters based on N,N'-ditridecyl-3,4,9,10-perylenetetracarboxylic diimide and pentacene," *Phys. Status Solidi - Rapid Res. Lett.*, vol. 2, no. 2, pp. 47–49, 2008.